RESEARCH ARTICLE

Enhanced Power Conversion Efficiency of Polymer Solar Cells Through Optimized Bilayer Tuning of PCBM and P3HT with Electron Blocking Layers PEDOT:PSS and Polyaniline

Kanhaiya Lal Mevta [1,2]**, Harish Kumar Meena** [1,2]**, Karishma Jain** [3]**, S. K. Jain** [3]**, Shalini Dixit** [1]**, Reena Verma** [1]**, Balram Tripathi** [1,*]

ABSTRACT: This study investigates the optimization of bilayer polymer solar cells (PSCs) using Poly(3-hexylthiophene) (P3HT) as the donor and [6,6]-phenyl-C61-butyric acid methyl ester (PCBM) as the acceptor. The active layers were prepared by spin coating at an optimized speed of 2000 rpm, followed by post-production annealing at 100°C. The electron-blocking layer (EBL) of PEDOT:PSS or polyaniline (PANI) was deposited under controlled conditions and annealed at 120°C for 15 minutes. Structural and morphological properties of the thin films were analyzed using X-ray diffraction (XRD), Fourier-transform infrared (FT-IR) spectroscopy, and scanning electron microscopy (SEM). Optical and electrical characteristics were evaluated using UV-Vis spectroscopy and Keithley electrometer under illumination. The results indicate that optimizing the thickness of the P3HT:PCBM bilayer significantly enhances the power conversion efficiency (PCE) by improving exciton dissociation and charge transport. SEM analysis revealed uniform film morphology, while XRD patterns showed distinct crystalline features, particularly for the P3HT layer. FT-IR spectra confirmed the successful deposition of the layers with characteristic functional groups. Electrical performance analysis demonstrated that annealing and bilayer thickness optimization reduced recombination losses, leading to higher short-circuit current density (Jsc) and open-circuit voltage (Voc). These findings emphasize the importance of layer thickness, morphology, and thermal processing in achieving efficient bilayer PSCs.

Keywords: P3HT/PCBM bilayer, Power conversion efficiency (PCE), Polymer solar cells, Optical and electrical properties.

1. INTRODUCTION

Polymer solar cells (PSCs), based on semiconductor and metal polymers, have garnered significant attention due to their low cost, flexibility, and potential for integration into printable energy devices [1, 2]. PSCs are typically classified into two types based on the structure of their active layers: single planar heterojunction (bilayer) and bulk heterojunction (BHJ) [3]. BHJ devices consist of a mixture of an electron-donor conjugated polymer (P-type) and an electron-accepting fullerene derivative (N-type) in the entire active layer volume, while bilayer devices have sequentially deposited layers of P-type and N-type materials [4, 5]. Conjugated polymers and fullerenes, when combined, segregate into separate nanoscale phases, forming a continuous network comprising polymer and fullerene components, which defines the BHJ structure [6, 7]. Light absorption in BHJ solar cells primarily occurs in the π-conjugated polymer, leading to the generation of tightly bound excitons. Studies have shown that excitons can diffuse

1   Department of Physics, S.S Jain Subodh P.G. College, An autonomous Institution, Jaipur -302004, India.
2   Department of Physics, University of Rajasthan Jaipur-302004, India.
3   Department of Physics, School of Physical Sciences, Manipal University Jaipur-302017, India.

*   Author to whom correspondence should be addressed:
    balramtripathi1181@gmail.com (Balram Tripathi)

only over a limited distance of approximately 10 nm [8, 9].

In recent years, advances in donor and acceptor materials have significantly improved the photoelectric conversion properties of the photoactive layer. Additive materials have been introduced to enhance donor/acceptor (D/A) heterojunction trapping abilities and optimize energy-level interface alignment [10, 11]. Among the most cost-effective and reproducible configurations of polymer-organic photovoltaic devices are BHJ solar cells containing a mixture of the semiconductor polymer P3HT and the organic fullerene derivative PCBM as the active layer, achieving average power conversion efficiencies (PCE) of up to ~5% [12, 13]. Moreover, flexible polymer-organic solar cells have been developed using various active-layer compositions deposited on plastic substrates [14, 15]. Poly(3-hexylthiophene) (P3HT) is a widely used donor material owing to its high hole transport ability (10^{-4}–10^{-2} cm² V^{-1} s^{-1}) and low bandgap. Meanwhile, [6, 6]-phenyl-C$_{61}$-butyric acid methyl ester (PCBM) is a promising acceptor material for heterojunction organic solar cells due to its excellent electron mobility and high stability.

The performance of organic solar cells depends on various factors during the fabrication process, such as film thickness, drying time, and annealing temperature. Controlling the film thickness and processing conditions of the active layer, where photons are absorbed to generate excitons, is crucial for achieving high short-circuit current and PCE [16]. Optimizing the thickness allows for a balance between optical absorption and series resistance of the active layer [17]. Additionally, thermal annealing improves the microstructure of the active layer, enhances the crystallinity of P3HT, and optimizes the PCBM-rich domain size, facilitating efficient electron transport across the interface [18].

To maximize energy conversion efficiency, solar cell parameters must be carefully investigated. Open circuit voltage (Voc), a key parameter, depends on the energy difference between the HOMO level of the donor material and the LUMO level of the acceptor material [19]. Short-circuit current density (Jsc), another critical factor, is influenced by the donor material's absorption properties, which are determined by its bandgap [20]. Structural modifications to reduce the bandgap or altering the active layer thickness can modify the Jsc. The fill factor (FF), which is influenced by Voc, Jsc, and active layer morphology, also plays a crucial role in determining the efficiency of organic solar cells [21].

The standardized efficiency of solar cells, or power conversion efficiency (PCE), is calculated from the current density versus voltage (J-V) characteristics of photovoltaic (PV) cells, as shown in Figure 1. The J-V curve is derived by measuring the current density output under simulated solar light over a variable voltage bias. The short-circuit current density (Jsc) is defined as the current density at zero bias, while the open circuit voltage (Voc) is the voltage at zero current. The FF is the ratio of the maximum power output to the product of Jsc and Voc [22].

PCE is calculated using the following equation:

$$PCE = \frac{P_{out}}{P_{in}} = \frac{J_{sc}V_{oc}FF}{P_{in}} \tag{1}$$

PCE represents the conversion efficiency of incident light power to usable electrical power. It depends on short-circuit current (Jsc), open circuit voltage (Voc), Fill factor (FF), and Incident power irradiance (Pin). Jsc, Voc, and FF can be directly measured from the I-V curve. Current density (J) is often used instead of current (I) to account for the device's active area. Precise measurement of the active area, especially for small-area PV devices, is essential for accurate efficiency calculations.

In this paper, we report on the optimization of power conversion efficiency (PCE) in polymer solar cells by systematically tuning the bilayer of PCBM and P3HT using an electron-blocking layer composed of PEDOT:PSS and polyaniline. We examine the impact of active layer thickness, annealing temperature, and device architecture on key performance parameters such as Jsc, Voc, FF, and overall PCE. The findings are supported by detailed experimental results, including J-V curve analysis, and demonstrate an effective strategy for enhancing the efficiency of polymer solar cells.

2. EXPERIMENTAL DETAILS

PEDOT:PSS solution (1 S/cm, 1.3 wt. % dispersion in H$_2$O) was purchased from Sigma-Aldrich. The concentration of PEDOT:PSS was 1.3% by weight, consisting of a 0.5 wt. % PEDOT and 0.8 wt. % PSS ratio. Polyaniline (PANI) emeraldine base (EB), with an average molecular weight (Mw) of 50,000, was also sourced from Sigma-Aldrich. PANI was dissolved in N-methyl-2-pyrrolidone (NMP) and sonicated for 15 minutes at room temperature to ensure complete dissolution.

Poly(3-hexylthiophene) (P3HT) solution, with a purity of 99.995%, and [6,6]-phenyl-C$_{61}$-butyric-acid-methyl ester (PCBM) (molecular weight: 910.88 g/mol) were purchased from Otto Chemie Pvt. Ltd. A 7 mg/ml concentration of P3HT and a 15 mg/ml concentration of PCBM solutions were prepared by dissolving each solute separately in toluene, using a magnetic stirrer for 12 hours at room temperature to achieve complete dissolution.

The bilayer heterojunction solar cells were fabricated by spin-coating the PEDOT:PSS/PANI, P3HT, and PCBM layers sequentially onto pre-cleaned glass substrates with indium tin oxide (ITO) films (1.2 × 1.2 cm²). The ITO substrates were cleaned using a multi-step process: initially, they were washed with acetone, followed by isopropyl alcohol (IPA), and finally, rinsed with deionized water. After cleaning, the substrates were subjected to UV-ozone treatment for 10 minutes to improve the surface wettability and adhesion of the subsequent layers.

Once the substrates were prepared, a uniform layer of PEDOT:PSS/PANI was spin-coated onto the ITO substrates at 3000 rpm for 30 seconds, followed by a 10-minute

annealing process at 100°C in a vacuum oven. This was followed by the deposition of the P3HT layer, spin-coated at 2000 rpm for 30 seconds, and the PCBM layer, spin-coated at 2000 rpm for 30 seconds as well. Both layers were annealed at 100°C for 30 minutes to optimize their crystallinity and morphology.

After the active layers were fabricated, the devices were transferred to a vacuum drying oven for further annealing at 100°C for 30 minutes to enhance the microstructure and the interfacial characteristics between the active layers. Finally, electrical contacts were made by depositing a conducting silver paste on the surface of the PCBM layer and the ITO electrodes to ensure good electrical contact. Current-voltage (I-V) characteristics of the fabricated devices were measured using a Keithley 2400 Electrometer under standard illumination conditions. The I-V measurements were recorded in a dark condition and under simulated sunlight at 100 mW/cm², and the results were used to calculate the power conversion efficiency (PCE) of the devices.

3. RESULTS AND DISCUSSION

3.1. Structural Analysis (XRD)

The X-ray diffraction (XRD) patterns of thin films of PCBM, P3HT, and layers of PCBM on the P3HT thin film are presented in Figure 1. The XRD patterns provide insights into the crystallinity and molecular arrangement of the materials. A prominent peak appears at a 2θ value of 23°, which corresponds to the (100) reflection plane of the thiophene rings in the crystalline chains of P3HT. This peak is a characteristic feature of P3HT's crystalline structure. The presence of this peak indicates that P3HT possesses a relatively ordered molecular structure, which is essential for charge transport in organic photovoltaics (OPVs). The observed peak is linked to the crystalline nature of P3HT, whereas the adjacent amorphous nature of PCBM, as indicated by the lack of distinct peaks, suggests that the PCBM is in an amorphous form when mixed with P3HT. This amorphous nature of PCBM can facilitate the formation of a mixed phase in the bilayer, which is beneficial for optimizing charge transport and reducing recombination losses in OPVs. The blending of crystalline P3HT with amorphous PCBM likely results in enhanced charge transfer at the interface, which is a critical factor for improving the device performance.

3.2. FT-IR Spectroscopy

The FT-IR spectra of PCBM, P3HT, and the layers of PCBM on P3HT thin film are shown in Figure 2. The FT-IR spectra provide valuable information about the functional groups and chemical bonding within the materials. In the FT-IR spectrum of P3HT, a broad absorbance is observed, indicating the presence of characteristic peaks associated with the polymer

backbone and side groups. Specifically, the peak at 2354 cm⁻¹ corresponds to the out-of-plane deformation of the C–H group in the aromatic ring, which is characteristic of thiophene-based polymers such as P3HT [23]. Additionally, the peaks around 2933 cm⁻¹ are assigned to the stretching vibrations of the aliphatic C–H group, which are typical for the side chains of P3HT. These features are consistent with the chemical structure of P3HT and confirm the successful deposition of P3HT onto the substrate [24].
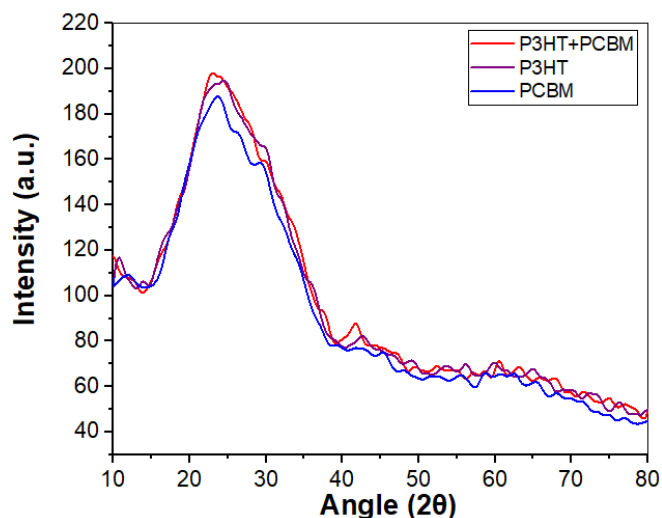

Fig. 2. XRD patterns of thin film of PCBM, P3HT and Layers of PCBM on P3HT thin film.
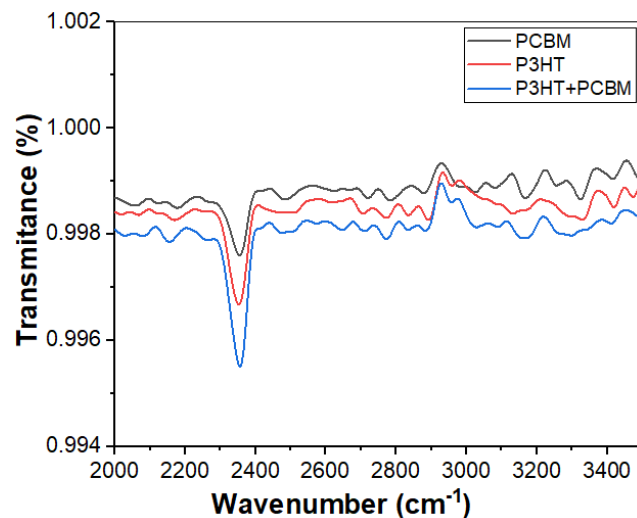

Fig. 2. FT-IR spectra for (a) PCBM (b) P3HT(c) Layers of PCBM on P3HT thin film.

For PCBM, the FT-IR spectra show distinct peaks associated with the carbonyl group (C=O) at around 1730 cm⁻¹, indicative of the fullerene derivative's presence. The interaction between P3HT and PCBM in the bilayer structure results in an overlapping of the spectra, with characteristic peaks from both materials appearing in the composite film.
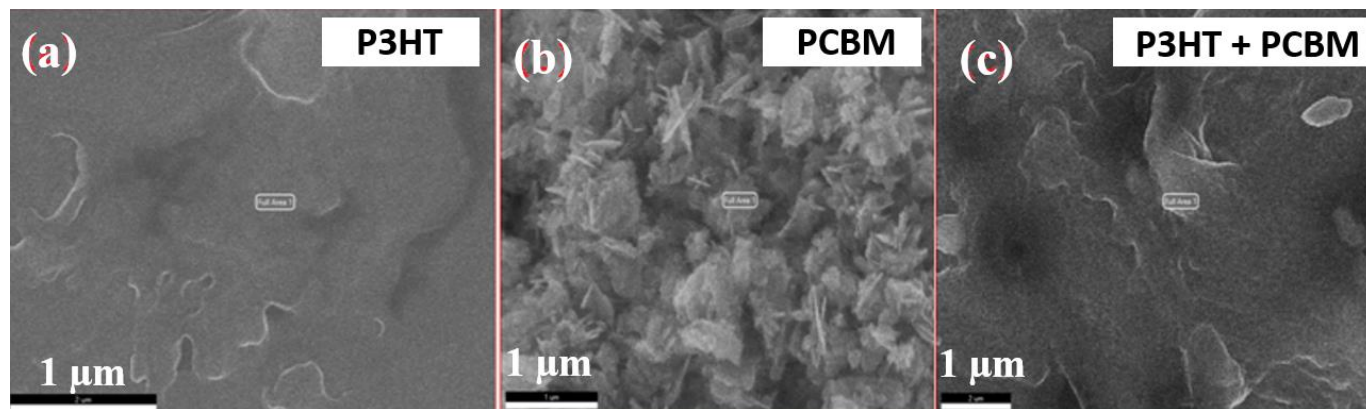
Fig. 3. SEM images of (a) PCBM (b) P3HT (c), Layers of PCBM on P3HT thin film.

This confirms the blending of PCBM and P3HT, which is crucial for efficient charge separation and transport within the device. The FT-IR results further support the successful fabrication of the bilayer thin film and provide a clearer understanding of the chemical interactions at the molecular level.

3.3. Surface Morphology

The surface morphology of PCBM, P3HT, and the layers of PCBM on P3HT thin films were investigated using scanning electron microscopy (SEM), as shown in Figure 3. The SEM images reveal distinct differences in the surface topography of the materials. The P3HT layer (Figure 3 (a)) exhibits a relatively smooth surface, characteristic of thin polymer films. The PCBM layer (Figure 3 (b)) shows a more uniform morphology, indicating good coverage of the substrate. When the PCBM layer is deposited on top of P3HT (Figure 3 (c)), a uniform and ordered arrangement of the polymer chains is observed. The interaction between P3HT and PCBM results in a well-mixed and less agglomerated polymer blend, likely due to the mono-dispersed electron spraying technique used during the deposition process. This uniformity ensures a large contact area between P3HT and PCBM, which is beneficial for charge transfer between the two materials.

The homogeneous blending of P3HT and PCBM is expected to minimize charge recombination losses and enhance the efficiency of charge separation and transport. The good dispersion of PCBM within the P3HT matrix also facilitates the formation of an efficient electron transport network, which is critical for achieving high photovoltaic performance in OPVs. Overall, the SEM results suggest that the bilayer films have desirable surface characteristics that promote efficient charge transfer, an important factor for high device performance.

3.4. Electrical (J-V) Characteristics

The electrical performance of the fabricated bilayer organic

photovoltaics (OPVs) was evaluated by measuring the current density-voltage (J-V) characteristics under simulated solar illumination (100 mW/cm²). The J-V curves of the various device configurations are shown in Figure 4. The power conversion efficiency (PCE) of the bilayer solar cells is influenced by several factors, including the thickness of the P3HT and PCBM layers, as well as the annealing temperature. The transient photovoltaic experiments revealed that the morphology of the bilayer structure differs from that of the bulk heterojunction (BHJ) structure. The bilayer configuration was found to be more favorable for reducing charge recombination compared to the BHJ structure. This is attributed to the well-defined interface between the P3HT and PCBM layers, which allows for efficient charge separation and minimizes the recombination of photogenerated carriers.
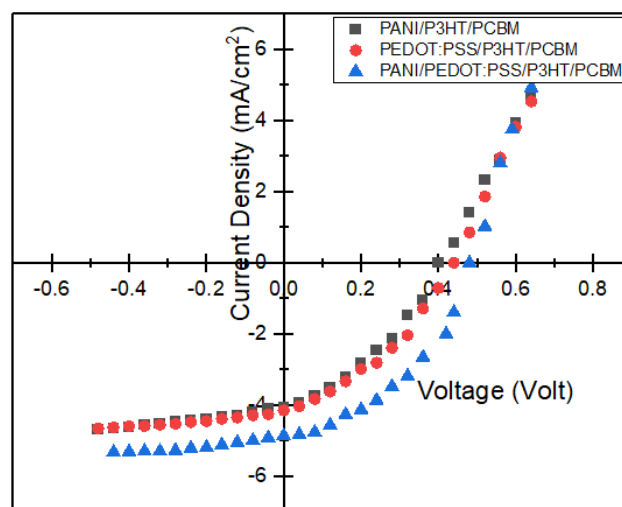

Fig. 4. *J-V* characteristics of (a) Layer of P3HT and PCBM on PANI Layer (b) Layer of P3HT and PCBM on PEDOT:PSS Layer (c), Layer of P3HT and PCBM on PANI and PEDOT:PSS Layer.

The J-V characteristics of the different bilayer OPVs are shown in Figure 4, where the device performance was measured under standard illumination conditions.

Table 1. J-V characterization of Bilayer of PCBM and P3HT OPV.

Sample	V_{oc}	J_{sc}	V_{max}	J_{max}	FF	PCE%
PANI/P3HT/PCBM	0.40	4.063	0.233	2.539	0.36	0.59
PEDOT:PSS/P3HT/PCBM	0.44	4.15	0.271	2.597	0.38	0.70
PANI/PEDOT:PSS/P3HT/PCBM	0.48	4.86	0.342	3.091	0.45	1.05

Table 1 presents the detailed J-V parameters of the devices, including the open-circuit voltage (Voc), short-circuit current density (Jsc), maximum voltage (Vmax), maximum current density (Jmax), fill factor (FF), and power conversion efficiency (PCE). Among the different device configurations, the bilayer OPV with PANI/PEDOT:PSS/P3HT/PCBM layers exhibited the highest PCE of 1.05%, with a Voc of 0.48 V, Jsc of 4.86 mA/cm², and a FF of 0.45. These values were higher than those of the PANI/P3HT/PCBM and PEDOT:PSS/P3HT/PCBM bilayer OPVs, which showed lower PCEs of 0.59% and 0.70%, respectively. The improved performance of the PANI/PEDOT:PSS/P3HT/PCBM device is likely due to the enhanced charge transport properties provided by the combination of PANI and PEDOT:PSS layers, which facilitate better carrier collection at the electrode interfaces [25, 26].

The increase in PCE for the PANI/PEDOT:PSS/ P3HT/PCBM device can be attributed to the improved energy level alignment between the electrode and the active layer, as well as the reduced series resistance and recombination losses. The results demonstrate that the optimization of the device architecture and material composition plays a crucial role in enhancing the performance of OPVs. The bilayer configuration, with its well-defined interface and optimized morphology, appears to be a promising approach for improving the efficiency of organic photovoltaic devices.

4. CONCLUSION

This study highlights the significant role of bilayer structure optimization in enhancing the performance of polymer solar cells (PSCs). By employing a bilayer heterojunction of P3HT and PCBM, the research focuses on achieving an ideal balance between optical absorption, exciton dissociation, and charge transport. The spin-coating technique at an optimized speed of 2000 rpm facilitated uniform film formation, while post-production annealing at 100°C improved the crystallinity and interfacial properties of the layers. Characterization using XRD, FT-IR spectroscopy, and SEM revealed key insights into the structural and morphological features of the films. XRD patterns confirmed the crystalline nature of the P3HT layer, which is critical for efficient charge transport, while FT-IR spectra validated the integrity of the thin films. SEM images highlighted a uniform morphology with minimal aggregation, indicating an improved donor-acceptor interface conducive to charge separation. Electrical characterization demonstrated that the thickness of the P3HT and PCBM layers, along with the annealing process, plays a

pivotal role in determining the photovoltaic performance. Optimized bilayer structures exhibited reduced charge recombination, leading to improved short-circuit current density (Jsc) and open-circuit voltage (Voc). Consequently, the power conversion efficiency (PCE) showed a notable enhancement compared to unoptimized configurations. The findings of this study underscore the potential of bilayer PSCs as a cost-effective and scalable approach for solar energy conversion. Future research could explore alternative electron-blocking layers and advanced annealing techniques to further enhance the efficiency and stability of PSCs. These advancements could pave the way for the widespread adoption of polymer-based photovoltaic technologies.

DECLARATIONS

Ethical Approval

We affirm that this manuscript is an original work, has not been previously published, and is not currently under consideration for publication in any other journal or conference proceedings. All authors have reviewed and approved the manuscript, and the order of authorship has been mutually agreed upon.

Funding

Not applicable

Availability of data and material

All of the data obtained or analyzed during this study is included in the report that was submitted.

Conflicts of Interest

The authors declare that they have no financial or personal interests that could have influenced the research and findings presented in this paper. The authors alone are responsible for the content and writing of this article.

Authors' contributions

All authors contributed equally in the preparation of this manuscript.

ACKNOWLEDGEMENTS

REFERENCES

[1] Brabec, C.J., Gowrisanker, S., Halls, J.J., Laird, D., Jia, S. and Williams, S.P., **2010.** Polymer–fullerene bulk-heterojunction solar cells. *Advanced Materials*, *22*(34), pp.3839-3856.

[2] Park, S.H., Roy, A., Beaupré, S., Cho, S., Coates, N., Moon, J.S., Moses, D., Leclerc, M., Lee, K. and Heeger, A.J., **2009.** Bulk heterojunction solar cells with internal quantum efficiency approaching 100%. *Nature Photonics*, *3*(5), pp.297-302.

[3] Yu, G., Gao, J., Hummelen, J.C., Wudl, F. and Heeger, A.J., **1995.** Polymer photovoltaic cells: enhanced efficiencies via a network of internal donor-acceptor heterojunctions. *Science*, *270*(5243), pp.1789-1791.

[4] Tang, C.W., VanSlyke, S.A. and Chen, C.H., 1989. Electroluminescence of doped organic thin films. *Journal of Applied Physics*, *65*(9), pp.3610-3616.

[5] Ayzner, A.L., Doan, S.C., Tremolet de Villers, B. and Schwartz, B.J., **2012.** Ultrafast studies of exciton migration and polaron formation in sequentially solution-processed conjugated polymer/fullerene quasi-bilayer photovoltaics. *The Journal of Physical Chemistry Letters*, *3*(16), pp.2281-2287.

[6] Günes, S., Neugebauer, H. and Sariciftci, N.S., **2007.** Conjugated polymer-based organic solar cells. *Chemical Reviews*, *107*(4), pp.1324-1338.

[7] Yang, C.Y. and Heeger, A.J., **1996.** Morphology of composites of semiconducting polymers mixed with C60. *Synthetic Metals*, *83*(2), pp.85-88.

[8] Shaw, P.E., Ruseckas, A. and Samuel, I.D., **2008.** Exciton diffusion measurements in poly (3-hexylthiophene). *Advanced Materials*, *20*(18), pp.3516-3520.

[9] Huijser, A., Savenije, T.J., Shalav, A. and Siebbeles, L.D., **2008.** An experimental study on the molecular organization and exciton diffusion in a bilayer of a porphyrin and poly (3-hexylthiophene). *Journal of Applied Physics*, *104*(3), p. 034505.

[10] Xu, Y.X., Chueh, C.C., Yip, H.L., Ding, F.Z., Li, Y.X., Li, C.Z., Li, X., Chen, W.C. and Jen, A.K.Y., **2012.** Improved charge transport and absorption coefficient in indacenodithieno [3, 2-b] thiophene-based ladder-type polymer leading to highly efficient polymer solar cells. *Advanced Materials*, *24*(47), pp.6356-6361.

[11] Albrecht, S., Tumbleston, J.R., Janietz, S., Dumsch, I., Allard, S., Scherf, U., Ade, H. and Neher, D., **2014.** Quantifying charge extraction in organic solar cells: the case of fluorinated PCPDTBT. *The Journal of Physical Chemistry Letters*, *5*(7), pp.1131-1138.

[12] Krebs, F.C., **2009.** Fabrication and processing of polymer solar cells: A review of printing and coating techniques. *Solar Energy Materials and Solar Cells*, *93*(4), pp.394-412.

[13] Das, A.J. and Narayan, K.S., **2013.** Retention of power conversion efficiency–from small area to large area polymer solar cells. *Advanced Materials*, *25*(15), pp.2193-2199.

[14] Youn, H., Park, H.J. and Guo, L.J., **2015.** Organic photovoltaic cells: From performance improvement to manufacturing processes. *Small*, *11*(19), pp.2228-2246.

[15] Gasparini, N., Salleo, A., McCulloch, I. and Baran, D., **2019.** The role of the third component in ternary organic solar cells. *Nature Reviews Materials*, *4*(4), pp.229-242.

[16] Ma, W., Yang, C., Gong, X., Lee, K. and Heeger, A.J., **2005.** Thermally stable, efficient polymer solar cells with nanoscale control of the interpenetrating network morphology. *Advanced Functional Materials*, *15*(10), pp.1617-1622.

[17] Chen, H.Y., Yang, H., Yang, G., Sista, S., Zadoyan, R., Li, G. and Yang, Y., **2009.** Fast-grown interpenetrating network in poly (3-hexylthiophene): methanofullerenes solar cells processed with additive. *The Journal of Physical Chemistry C*, *113*(18), pp.7946-7953.

[18] Reyes-Reyes, M., Kim, K. and Carroll, D.L., **2005.** High-efficiency photovoltaic devices based on annealed poly (3-hexylthiophene) and 1-(3-methoxycarbonyl)-propyl-1-phenyl-(6, 6) C61 blends. *Applied Physics Letters*, *87*(8).

[19] Brabec, C.J., Sariciftci, N.S. and Hummelen, J.C., **2001.** Plastic solar cells. *Advanced Functional Materials*, *11*(1), pp.15-26.

[20] Bartelt, J.A., Beiley, Z.M., Hoke, E.T., Mateker, W.R., Douglas, J.D., Collins, B.A., Tumbleston, J.R., Graham, K.R., Amassian, A., Ade, H. and Fréchet, J.M., **2013.** The importance of fullerene percolation in the mixed regions of polymer–fullerene bulk heterojunction solar cells. *Advanced Energy Materials*, *3*(3), pp.364-374.

[21] Ratier, B., Nunzi, J.M., Aldissi, M., Kraft, T.M. and Buncel, E., **2012.** Organic solar cell materials and active

layer designs—improvements with carbon nanotubes: a review. *Polymer International*, *61*(3), pp.342-354.

[22] Green, M.A., Emery, K., King, D.L., Hisikawa, Y. and Warta, W., **2006.** Solar cell efficiency tables (version 27). *Progress in Photovoltaics*, *14*(1), pp.45-52.

[23] Mikroyannidis, J.A., Kabanakis, A.N., Sharma, S.S. and Sharma, G.D., **2011.** A simple and effective modification of PCBM for use as an electron acceptor in efficient bulk heterojunction solar cells. *Advanced Functional Materials*, *21*(4), pp.746-755.

[24] Kalita, G., Masahiro, M., Koichi, W. and Umeno, M., **2010.** Nanostructured morphology of P3HT: PCBM bulk heterojunction solar cells. *Solid-State Electronics*, *54*(4), pp.447-451.

[25] Lee, J.U., Jung, J.W., Emrick, T., Russell, T.P. and Jo, W.H., **2010.** Synthesis of C 60-end capped P3HT and its application for high performance of P3HT/PCBM bulk heterojunction solar cells. *Journal of Materials Chemistry*, *20*(16), pp.3287-3294.

[26] Lin, X., Seok, J., Yoon, S., Kim, T., Kim, B. and Kim, K., **2014.** Morphological investigation of P3HT/PCBM heterojunction and its effects on the performance of bilayer organic solar cells. *Synthetic Metals*, *196*, pp.145-150.